ARMY RESEARCH LABORATORY

Traction Launch of Scaled Laboratory Kinetic Energy Penetrators

Brett R. Sorensen

ARL-TR-798 July 1995

NOTICES

Destroy this report when it is no longer needed. DO NOT return it to the originator.

Additional copies of this report may be obtained from the National Technical Information Service, U.S. Department of Commerce, 5285 Port Royal Road, Springfield, VA 22161.

The findings of this report are not to be construed as an official Department of the Army position, unless so designated by other authorized documents.

The use of trade names or manufacturers' names in this report does not constitute endorsement of any commercial product.

REPORT DOCUMENTATION PAGE

Form Approved
OMB No. 0704-0188

1. AGENCY USE ONLY *(Leave blank)*	2. REPORT DATE	3. REPORT TYPE AND DATES COVERED
	July 1995	Final, October 1991 - June 1992

4. TITLE AND SUBTITLE

Traction Launch of Scaled Laboratory Kinetic Energy Penetrators

5. FUNDING NUMBERS

PR: 1L162618AH80

6. AUTHOR(S)

Brett R. Sorensen

7. PERFORMING ORGANIZATION NAME(S) AND ADDRESS(ES)

U.S. Army Research Laboratory
ATTN: AMSRL-WT-TC
Aberdeen Proving Ground, MD 21005-5066

8. PERFORMING ORGANIZATION REPORT NUMBER

ARL-TR-798

9. SPONSORING / MONITORING AGENCY NAME(S) AND ADDRESS(ES)

10. SPONSORING / MONITORING AGENCY REPORT NUMBER

11. SUPPLEMENTARY NOTES

12a. DISTRIBUTION / AVAILABILITY STATEMENT

Approved for public release; distribution is unlimited.

12b. DISTRIBUTION CODE

13. ABSTRACT *(Maximum 200 words)*

This report discusses the design, analysis, and testing phases of a modification in subscale, kinetic energy projectile technology. Typically, subscale penetrators are push launched, while the actual full-scale penetrators are traction launched. This condition was acceptable until recently when push launch technology could no longer fully satisfy the needs of the researcher. Therefore, a technique for implementing traction launch technology into the subscale laboratory environment was needed. This report presents the theory, finite element analysis, and actual testing of one concept. The design process was highlighted by the use of several finite elements codes (implicit and explicit) and the exceptional agreement between the results.

14. SUBJECT TERMS	15. NUMBER OF PAGES
sabot, finite element analysis, kinetic energy penetrators, sabot design	26
	16. PRICE CODE

17. SECURITY CLASSIFICATION OF REPORT	18. SECURITY CLASSIFICATION OF THIS PAGE	19. SECURITY CLASSIFICATION OF ABSTRACT	20. LIMITATION OF ABSTRACT
UNCLASSIFIED	UNCLASSIFIED	UNCLASSIFIED	UL

INTENTIONALLY LEFT BLANK.

TABLE OF CONTENTS

INTENTIONALLY LEFT BLANK.

LIST OF FIGURES

INTENTIONALLY LEFT BLANK.

1. INTRODUCTION

The most effective weapon of the modern tank against heavy armor threats is the kinetic energy (KE) projectile (Figure 1). This projectile consists of a subcaliber penetrator which is carried through the cannon by a multipetal sabot. The high inertial loads of the penetrator are transmitted to the sabot via a geometric traction interface (i.e., annular buttress grooves and/or a threaded friction drive).

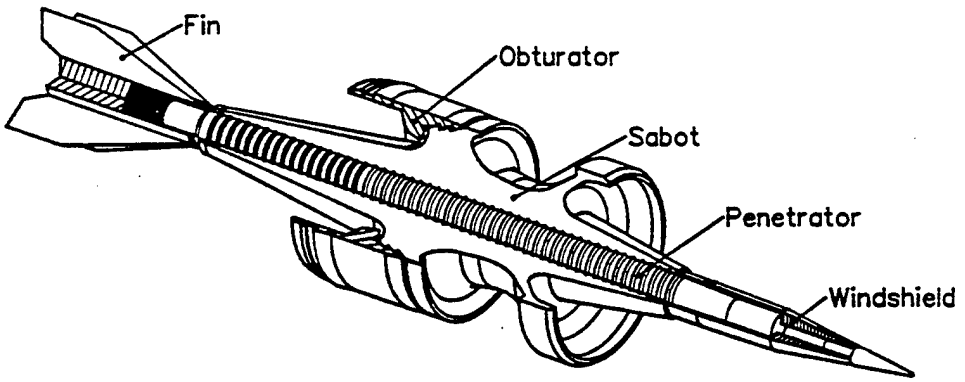

Figure 1. An isometric view of a fielded kinetic energy projectile.

However, in a research environment where one-quarter and one-third scale work is often performed, these shear transferring mechanisms present several distinct disadvantages. Complex penetrator geometry can require additional complexity in the sabot with increased manufacturing costs for the projectile. Due to integration and manufacturing considerations, some of the groove characteristics cannot be faithfully scaled; the typical affect is an increase in the percentage of groove mass with respect to the entire penetrator mass. Furthermore, since subscale tests are typically used to examine phenomenological trends, the presence of grooves can greatly increase the complexity of an analysis and can mask important factors.

Reducing the previous arguments to cost and simplicity, subscale penetrators have traditionally been right circular cylinders (except for different nose shapes) and are push launched. However, if the combination of penetrator geometry and material properties prohibit a push launch, a traction sabot becomes necessary. (Figure 2 illustrates the conceptual differences between push and traction launch

technology.) Therefore, a study was performed to design a sabot and a penetrator-sabot interface which would minimize the interface geometry for these subscale projectiles.

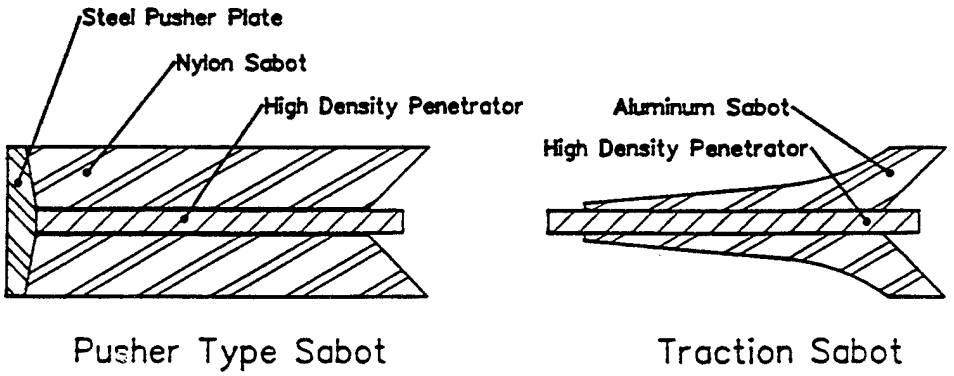

Figure 2. Comparison between push-launch and traction-launch sabot technology.

2. THEORY

The simplest form of traction is friction. However, it is not intuitively obvious that frictional forces alone can hold the penetrator in the sabot when the assembly is experiencing 50,000–150,000 g's of acceleration. Yet, the simplicity of the solution is attractive enough to merit further investigation.

As with any new design effort, simplifying assumptions are made and free body diagrams are generated to provide insight and governing equations for the problem. The geometry assumptions used in this analysis are that the penetrator is a cylinder and the sabot is a frustum (Figure 3). It is also assumed that the sabot fills the bore of the cannon and a pressure P is accelerating the projectile at $\ddot{z}$. The free body diagrams for each body appear in Figure 4.

Since the projectile is axisymmetric, radial forces cancel out, leaving force balances on the axial forces only. Using Newton's Second Law, force balances on the penetrator and sabot yield Equations 1 and 2, respectively. For the frictional concept to work, the acceleration of each body must be equal, and the same as the acceleration of the system. Performing a force balance on the system, the internal forces cancel, and Equation 3 is obtained.

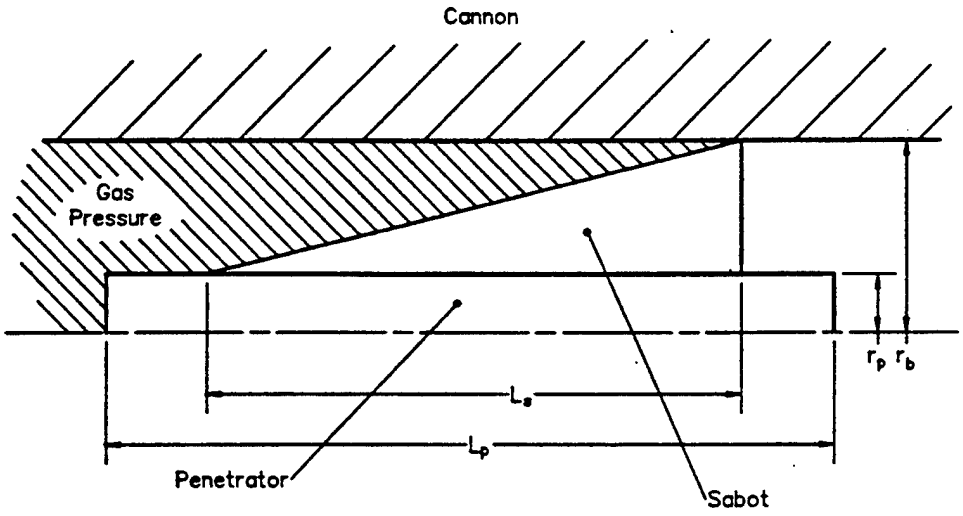

Figure 3. Simplified projectile model.

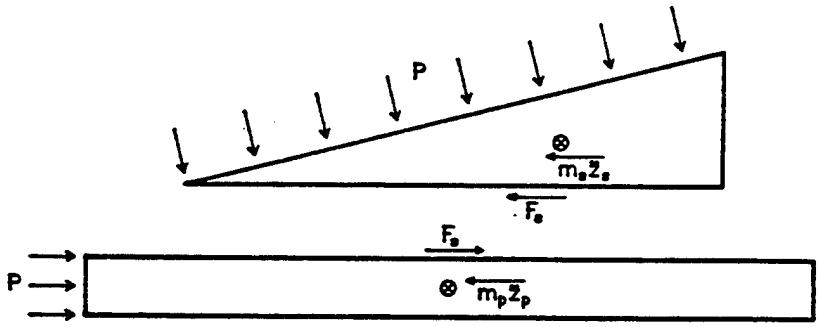

Figure 4. Free body diagrams.

$$m_p \ddot{z}_p = \pi r_p^2 P + F_s \tag{1}$$

$$m_s \ddot{z}_s = \pi (r_b^2 - r_p^2) P - F_s \tag{2}$$

$$\ddot{z}_s = \ddot{z}_p = \ddot{z} = \frac{\pi r_b^2 P}{m_s + m_p} \tag{3}$$

where,

$m_p \equiv$ penetrator mass

$m_s \equiv$ sabot mass

$\ddot{z}_p \equiv$ acceleration of penetrator c.g.

$\ddot{z}_s \equiv$ acceleration of sabot c.g.

$r_p \equiv$ penetrator radius

$r_b \equiv$ barrel radius

$P \equiv$ pressure

$F_s \equiv$ interface shear force

By subtracting Equation 2 from Equation 1 and removing the acceleration term by substitution of Equation 3, the governing equation can be written in terms of component masses, m_s and m_p, penetrator radius, r_p, barrel radius, r_b, pressure, P, and the term specifying the shear force between the bodies, F_s. It is the expression for the shear forces which will dictate the feasibility of the concept. To reduce Equation 4 into its fundamental parameters, Equations 5 and 6 provide the mass relationships for both the penetrator and the sabot. Equation 7 provides the physical foundation for F_s.

$$(m_p - m_s)\frac{\pi r_b^2 P}{m_s + m_p} = \pi P (2 r_p^2 - r_b^2) + 2 F_s \tag{4}$$

$$m_p = \pi r_p^2 L_p \rho_p \tag{5}$$

$$m_s = \frac{\pi}{3} L_s (r_b^2 + r_p r_b - 2 r_p^2) \rho_s \tag{6}$$

$$F_s = 2 \pi r_p L_s \bar{\sigma}_r \mu \tag{7}$$

where,

$\rho_p \equiv$ penetrator density

$\rho_s \equiv$ sabot density

$L_p \equiv$ penetrator length

$L_s \equiv$ sabot length

$\bar{\sigma}_r \equiv$ average radial stress at the interface

$\mu \equiv$ static coefficient of friction

less than 1.0 produces a feasible design since the required sabot length is less than the penetrator length. As mentioned earlier, the designer has some control over f, so it was also varied to provide a family of curves.

The results of this analysis are provided in Figure 5 for penetrator aspect ratios of 20, 30, and 40 for a 50-mm cannon. Materials used in the analysis were tungsten heavy alloy (WHA) for the penetrator and aluminum for the sabot, with densities of 17,600 and 2,700 kg/m^3, respectively. These results show that for $f \geq 0.3$, the concept is feasible if the assumptions are valid.

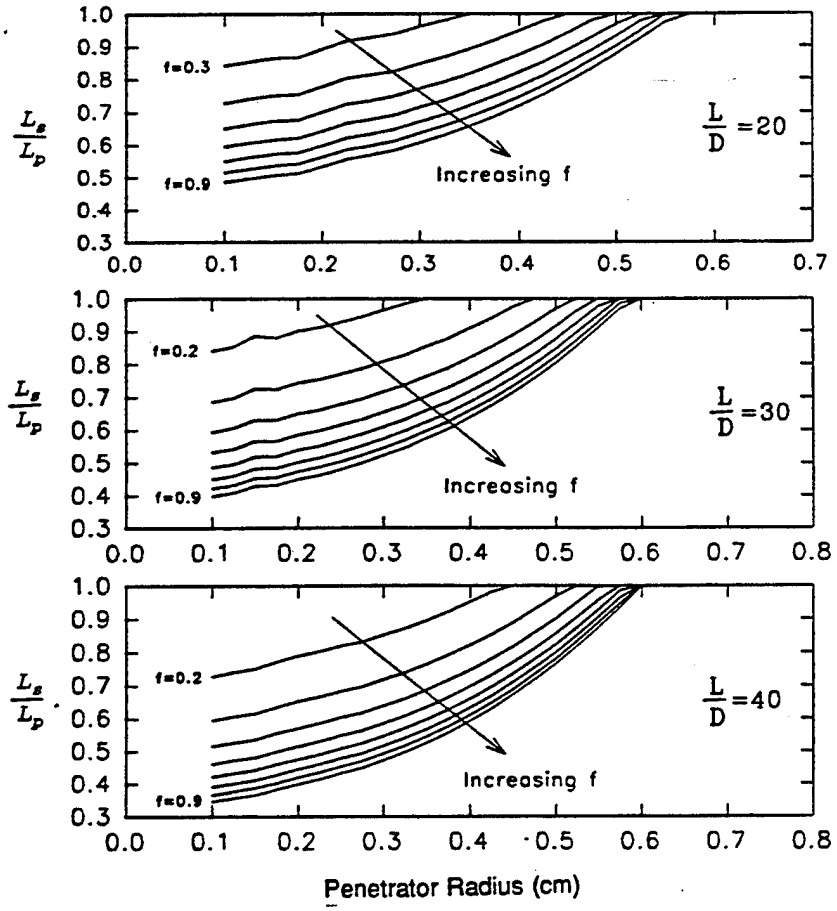

Figure 5. Results from Equation 8 representing minimum sabot length, normalized by penetrator length, to successfully launch a penetrator of a given radius from a 50-mm cannon.

In Equation 7, the term $2\pi r_p L_s$ represents the area of the interface between the sabot and the penetrator, μ is the coefficient of friction, and $\bar{\sigma}_r$ is the average radial stress at the interface. Assuming that the penetrator geometry is defined, F_s is a function of sabot length, L_s, interface stress, $\bar{\sigma}_r$, and the coefficient of friction, μ. $\bar{\sigma}_r$ is a function of sabot shape, material selections, and pressure, all of which the designer has some degree of control over. μ is a physical constant which is a function of the materials and surface quality. Therefore, the only remaining unknown is L_s. Substituting Equations 5–7 into Equation 4 and solving for L_s provides:

$$A L_s^2 + B L_s + C = 0 \tag{8}$$

where,

$$A = \frac{4\pi}{3} \rho_s (r_b^2 + r_p r_b - 2 r_p^2) r_p \frac{\bar{\sigma}_r}{P} \mu \tag{8a}$$

$$B = \frac{2\pi}{3} \rho_s (r_b^2 + r_p r_b - 2 r_p^2) r_p^2 + 4 \pi r_p^3 L_p \rho_p \frac{\bar{\sigma}_r}{P} \mu \tag{8b}$$

$$C = 2\pi r_p^2 L_p \rho_p (r_p^2 - r_b^2) \tag{8c}$$

The values for r_p, L_p, ρ_p, ρ_s, and r_b are constants. The terms $\bar{\sigma}_r$, P, and μ are parameters which the designer can use to control L_s. For analysis purposes, these three terms are lumped together as term f.

$$f = \frac{\bar{\sigma}_r}{P} \mu \tag{9}$$

To determine the feasibility of the concept, the following parametric study was proposed. The variables ρ_p, ρ_s, and r_b were defined for a system of interest. To study an entire class of penetrators, aspect ratio (L/D) was defined. Equation 8 was then solved by holding f constant and varying r_p over the range of interest. To provided a measure of goodness to L_s, it was normalized by L_p; thus, any result

3. ANALYSIS

The remaining portion of this report will concentrate on verification of the theory through finite element and experimental methods. To limit the scope of this initial finite element study, only one cannon bore diameter will be examined—50 mm.

Because of the nature of the curves in Figure 5, the parametric analysis capabilities in ANSYS (DeSalvo and Gorman) were especially useful in examining the assumptions made earlier. A parametric model of Figure 3 was constructed in ANSYS, and more than 100 different projectile geometries were examined by varying L_p and r_p and calculating L_s. For the purpose of this study, f was assumed to be 0.3. The finite element model was axisymmetric and the solution was performed quasi-statically (Drysdale 1981). Nodes along the penetrator-sabot interface were shared to form a simple bimetallic interface. Proper boundary conditions, pressure and acceleration, were computed and applied for each set of geometry. In addition, one node on the penetrator was fixed in the axial direction, as required for an axisymmetric, static solution.

Using the results from these analyses, two points can be made. First, the expression $f = 0.3$ can be checked for validity. The coefficient of friction is a physical constant; therefore, only the expression $\bar{\sigma}_r/P$ needs to be evaluated. For each configuration, $\bar{\sigma}_r$ along the material interface was computed. By choosing a reasonable value for μ, f can now be defined. Results of the parametric analysis put $\bar{\sigma}_r$ at 120–150% of P (Table 1). From handbook tables (Oberg, Jones, and Horton 1985), μ is at least 0.3–0.4; therefore, a value of f ~0.3–0.5 is reasonable to expect and, according to Figure 5, many penetrator configurations exist for the specifications originally set forth.

In addition to examining the relationship between $\bar{\sigma}_r$ and P along the sabot/penetrator interface, another relationship exists between the radial and shear forces. Even though the nodes on the material interface are shared, significant information can be extracted. By comparing the product of the radial stress and coefficient of friction, σ,μ, to the shear stress, τ, the status of a sliding interface can be inferred. If the product of the coefficient of friction and the radial stress is larger than the shear stress, sufficient traction exists to accelerate the penetrator and sabot together. To provide a measure between the two parameters, each was plotted along the length of the sabot (Figure 6) for a group of penetrators (L/D = 30). Figure 6 illustrates that adequate traction exists to accelerate both bodies together.

Table 1. Result of $\bar{\sigma}_r/P$

R (m)	L/D				
	20	25	30	35	40
0.0020	1.64	1.54	1.48	1.42	1.40
0.0025	1.47	1.41	1.37	1.34	1.31
0.0030	1.38	1.34	1.31	1.28	1.26
0.0035	1.32	1.29	1.27	1.25	1.23
0.0040	1.29	1.26	1.24	1.22	1.22
0.0045	1.26	1.24	1.22	1.21	1.21
0.0050	1.24	1.22	1.21	1.20	1.20
0.0055	1.22	1.21	1.20	1.20	1.21
0.0060	1.21	1.20	1.19	1.20	1.20
0.0065	1.20	1.19	1.18	1.19	1.19
0.0070	1.19	1.18	1.19	1.19	1.19

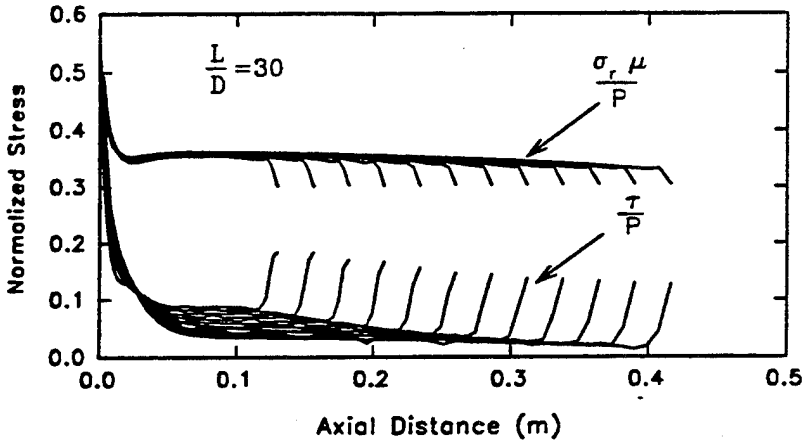

Figure 6. Comparison of normalized radial and shear stress along the penetrator-sabot interface for L/D 30 penetrators.

Although the results of the previous analyses tend to support the initial premise that frictional forces alone will provide sufficient traction to the penetrator, two significant assumptions were made: the penetrator-sabot interface used shared nodes and the analyses were quasi-static. To continue toward a final

design and manufacture projectiles would be imprudent until these assumptions were removed. Therefore, a dynamic analysis with some model of the sliding interface was necessary.

To conduct a dynamic analysis in ANSYS was very difficult with the present capabilities. ANSYS Revision 4.4A has the necessary capabilities to model the sliding interface by using the 2-D interface element (STIF12). However, the introduction of friction adds nonconservative forces into the analysis and the rate at which loading occurs (from 0 to 400 MPa in 2 ms) forces an extremely small time step to ensure convergence. Providing a mesh which would accurately resolve the stresses would severely tax the workstation which ANSYS is resident to the point where one analysis would take days or even weeks to complete. Therefore, the NIKE2D and DYNA2D hydrocodes were utilized in a supercomputer environment. NIKE2D and DYNA2D (Hallquist 1983, 1986, 1988) are two hydrocodes which were developed at the Lawrence Livermore National Laboratory to solve dynamic problems. The codes are similar with the exception of their integration algorithms; NIKE is implicit and DYNA is explicit. Both codes have been vectorized to execute efficiently in the CRAY environment and can also resolve sliding interfaces more efficiently than ANSYS (Rev 4.4A) can.

To demonstrate that the sabot concept works, prototype projectiles needed to be manufactured and tested. To work towards this objective, the remaining finite element modeling efforts focus on the candidate projectile. The penetrator is cylindrical with a length of 0.24 m and a diameter of 0.008 m. The sabot length was determined from Equation 8 using a value of 0.3 for f. This is a conservative value for f, but the increased margin was desirable due to the novelty of the work.

The finite element mesh used in the NIKE and DYNA analyses is displayed in Figure 7. Both programs were used to provide confidence that different solution techniques yielded similar results. In both models, slidelines with voids and friction ($\mu = 0.3$) were utilized. Figure 8 displays the resulting displacement, velocity, and acceleration curves for the penetrator from the NIKE analysis. Although these curves provide information to compare to the DYNA analysis, the most telling information is penetrator displacement relative to the sabot (Figure 9). These curves show the relative axial displacement between the penetrator and the sabot at the three locations indicated. The results show that even though there is relative displacement, it is small enough to be inconsequential. To be complete, the results of the DYNA analysis are also presented (Figure 10). The agreement between the two solutions is quite good. For the location at the front of the sabot, there is a 7% difference in the maximum relative displacement and a

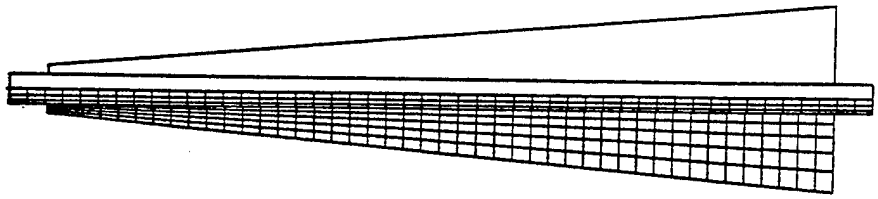

Figure 7. Mesh used in the NIKE and DYNA analyses.

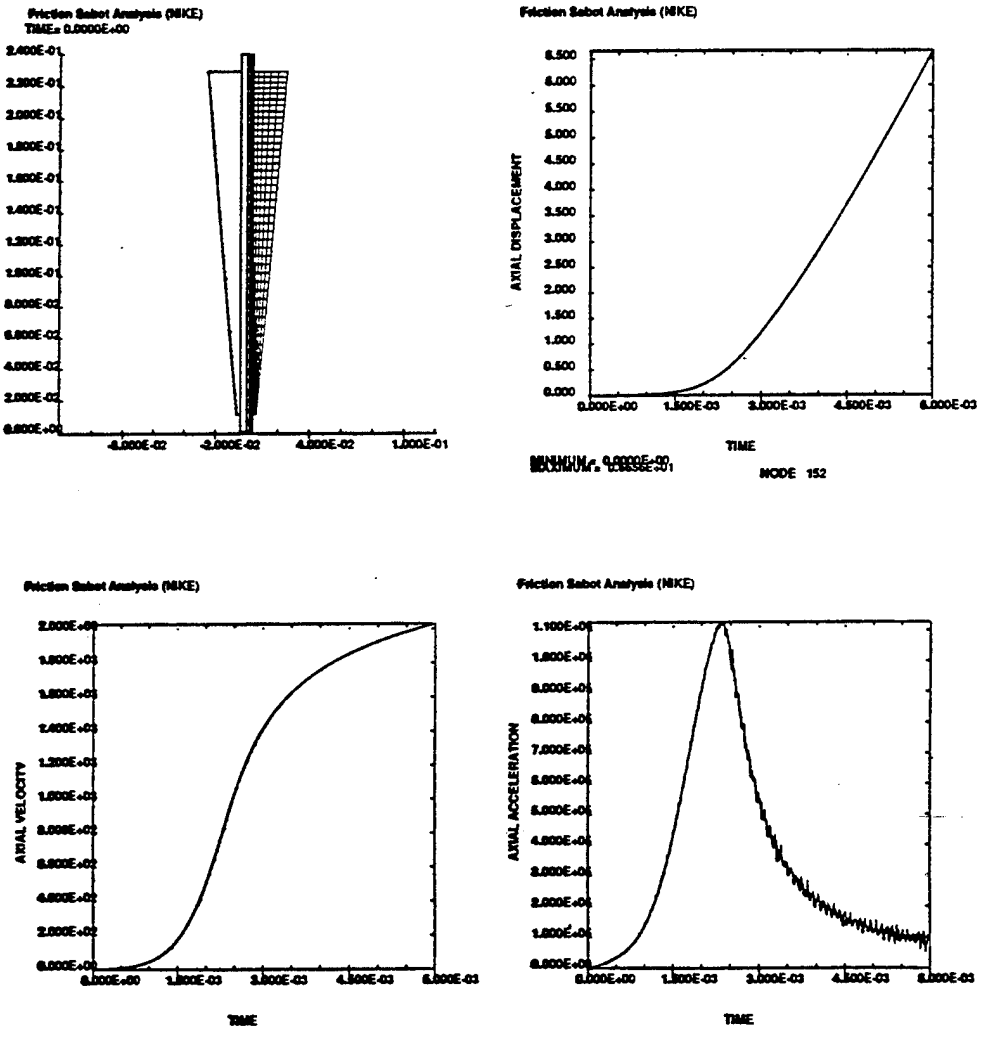

Figure 8. Displacement, velocity, and acceleration histories from NIKE.

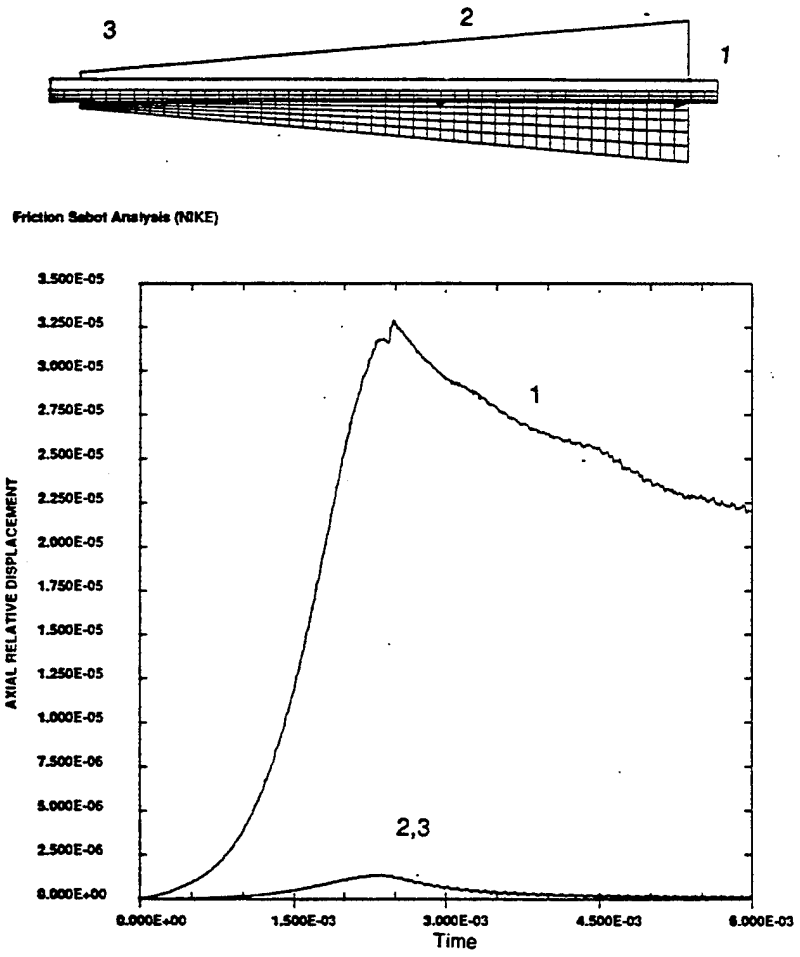

Figure 9. Relative displacement between nodes on the penetrator and the sabot at three different locations. (NIKE analysis, ITS = 5.0E-6.)

slight difference in the shape of the curve beyond the maximum. This is acceptable when considering that the integration time step in DYNA was an order of magnitude smaller.

The difference between curve 1 and curves 2 and 3 in Figure 9 and 10 is explained in Figure 11. This figure shows two curves, the product of the normal interface force and the coefficient of friction ($F_n \mu$) and the tangential interface force (F_s) as a function of axial distance from the front of the sabot. This graph shows that a small part of the interface does not have sufficient normal force to prevent sliding; therefore, the front of the sabot has a larger relative displacement. This was also the case with the quasi-static results from ANSYS shown in Figure 5. In the ANSYS analysis, examination of the front of the sabot shows that the shear stress is larger than the product of the radial stress and the coefficient of

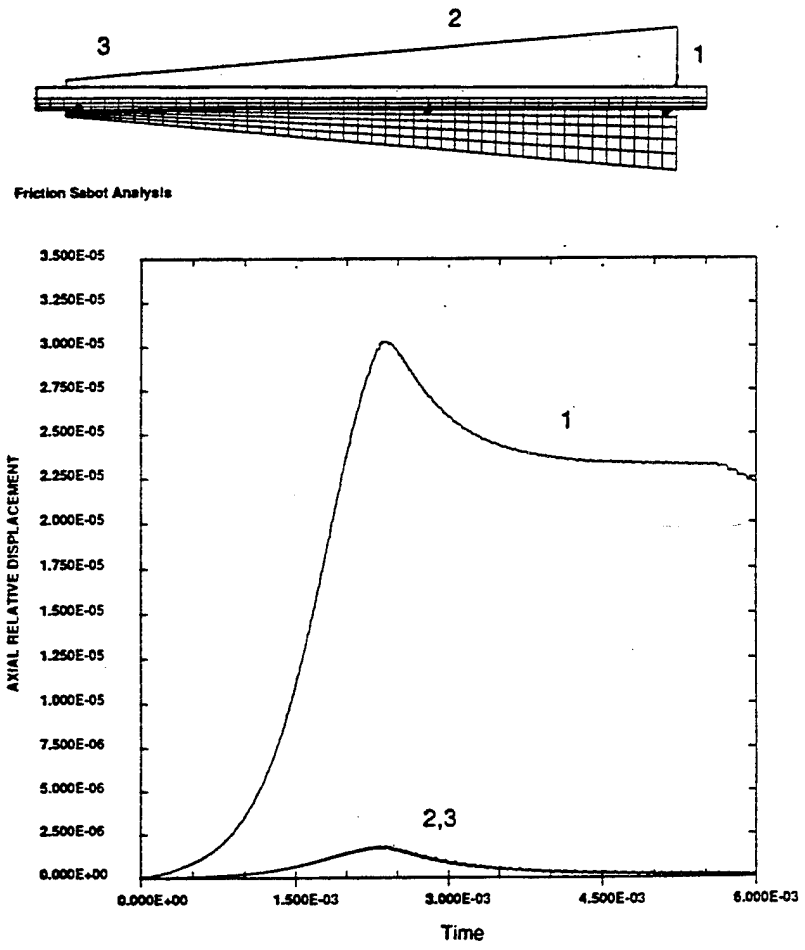

Figure 10. Relative displacement between nodes on the penetrator and the sabot at three different locations. (DYNA analysis, ITS = 5.0E-7.)

friction; therefore, if the nodes along the interface were not shared, slippage would occur. In the ANSYS analysis, the shear stress was higher and more localized because the nodes were shared and slippage could not occur as in the NIKE and DYNA analyses.

Based on the successful result of the dynamic analyses, a final sabot design was developed. This design incorporated all of the features necessary to interact with the cannon in an appropriate manner, be mass efficient, and not violate any of the initial assumptions. Two conditions which must be met within the cannon are stability and a seal to prevent gas leakage. A third condition must also be met at muzzle exit, a means to use aerodynamic forces to separate the sabot from the penetrator. Finally, the sabot must be inexpensive to manufacture. To maintain stability in the cannon, the sabot must have one contact point

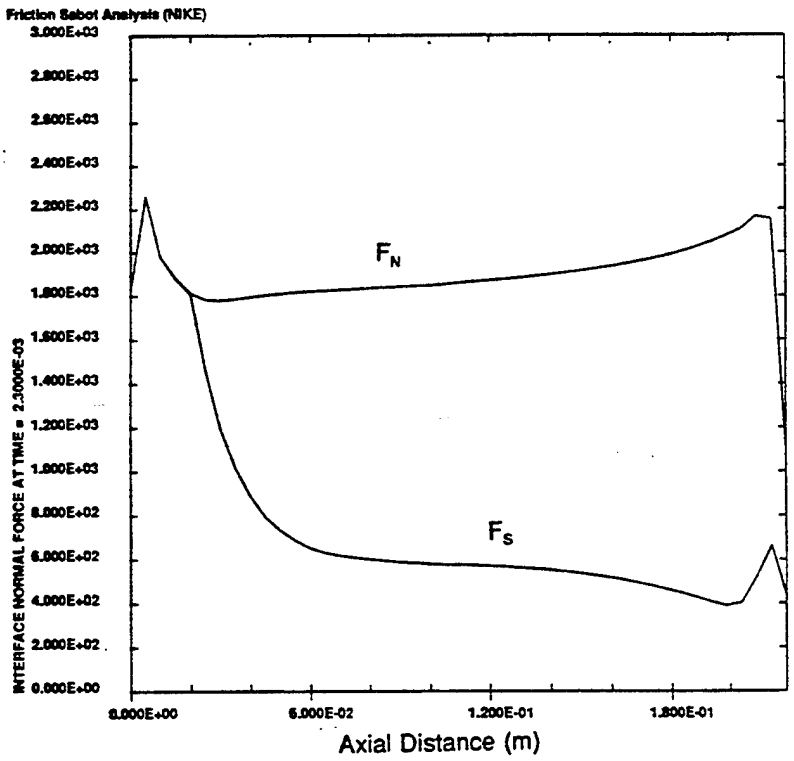

Figure 11. Sabot-penetrator interface forces at peak pressure.

at least two-thirds the bore diameter in length or two contact points separated by this distance. Because the sabot must be a single-ramp design (initial assumption), only one bore riding surface is possible. The required aerodynamic discard forces are generated by incorporating a scoop within the bore riding surface. Finally, a high-pressure seal is formed by machining notches into the bore riding surface and inserting nylon bands. By making the diameter of the nylon bands larger than the bore and pressing the projectile into the cannon, an effective seal is provided. Figure 12 shows a sketch of the proposed final design, illustrating the incorporation of the above details.

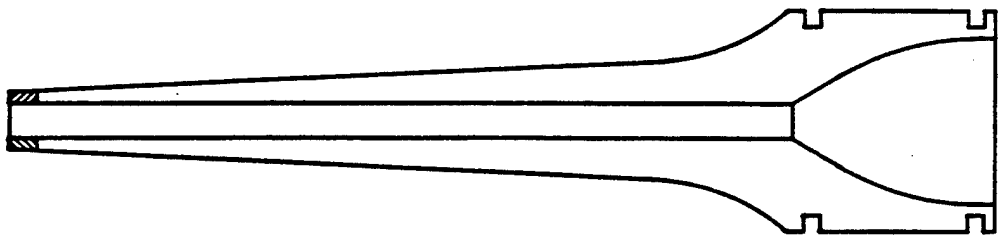

Figure 12. Final sabot concept.

Now that the sabot design has been conceptualized, final dimensions are required. To provide this information and minimize mass while ensuring that stresses did not exceed yield criteria, a parametric, quasi-static analysis was conducted in ANSYS. The groove details for the nylon bands were removed and a parametric model was generated for the sabot profile. The analysis was performed quasi-statically because dynamics were not a concern in determining the stress distribution within the projectile. Furthermore, since the sabot mass must be below a specified threshold and not the absolute minimum, the optimization algorithm was not utilized. The final stress results for the projectile for the quasi-static ANSYS analysis are presented in Figure 13. Also plotted are the NIKE results for the same projectile at peak pressure for a dynamic solution. The correlation between solutions is excellent, providing adequate verification of the results.

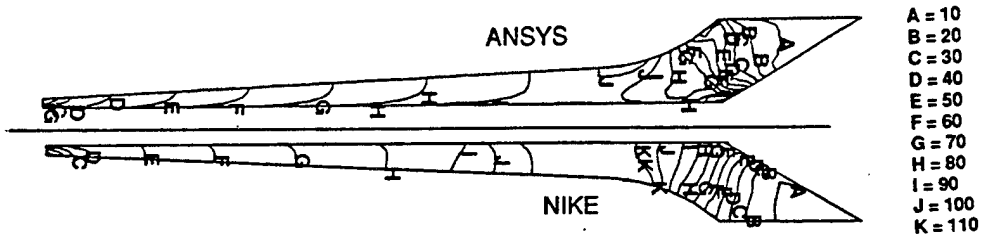

Figure 13. Effective stress contour plot of the final sabot design. Both ANSYS and NIKE results are presented in percentage of yield stress.

Two issues remain to be discussed—discarding the sabot at muzzle exit and manufacturing. To discard the sabot, it must be split into at least two parts along the axis of symmetry. This will permit the aerodynamic forces to separate the sabot from the penetrator. This poses several problems. First, if the sabot is in multiple pieces, there are more than two independent bodies which must be kept together while accelerating through the cannon. Second, manufacturing costs will increase. Finally, there is no static mechanism to hold the penetrator in the sabot prior to the launch sequence. To solve these problems, the following strategy was proposed. The sabot would be turned on a lathe in one piece. The inside details would be completed first, leaving a 0.02–0.04 mm interference with the penetrator at the aft end of the sabot. Once the turning operations were complete, wire EDM technology would be used to place one (or two orthogonal) splits in the sabot along the axis. These splits would start at the front of the sabot and extend to the aft, leaving 6–10 mm of length uncut. In this region, an interference fit with the penetrator would generate sufficient radial stress to hold the two components together while handling the projectile. To prevent gas from passing through the splits, a RTV (silicone rubber) seal was placed on the projectile in a manner to prevent any RTV from getting into the splits.

The only question remaining to be answered is how will the sabot break at discard? Will fracture occur along the axis of symmetry on each split, or will the fracture plane be perpendicular to the axis of symmetry? The desirable fracture plane is parallel to the axis of symmetry, but it is unknown whether this will happen. As a stress concentration exists due to the splits, the hypothesis is that fracture will continue in the direction of the splits. However, this will not be known until after initial testing has occurred.

4. TEST RESULTS

Two projectiles of two separate designs were tested for a total of four tests. The difference between the two designs was simply a manufacturing detail; all four projectiles had two orthogonal splits, but two were created by wire EDM and two by a band saw. The only substantial difference being the kerf for the band saw was much larger. A photograph of a projectile is presented in Figure 14. The front of the projectile is on the right and one of the splits is clearly evident. The two annular bands on the forward portion of the sabot are the nylon obturation bands. The penetrator is flush with the front of the sabot and extends past the aft end of the sabot.

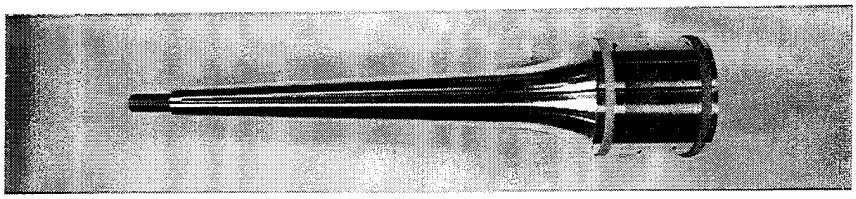

Figure 14. Photograph of the projectile.

The launch conditions for each test were kept similar. The maximum breech pressure was approximately 400 MPa, resulting in a maximum acceleration of 100,000 g's and a muzzle velocity of 1,650 m/s. A later test entry will increase the pressure to the cannon's upper limit of 650 MPa, resulting in a muzzle velocity in excess of 2,000 m/s. Of four tests, three were successful. The unsuccessful test was the first projectile with the band saw splits. In this test, the penetrator experienced setback and separated from the sabot while in-bore. One hypothesis for this traction failure the splits in the sabot were not deburred well enough, minimizing the contact area between the penetrator and sabot.

The confirmation of the concept working is provided by flash radiography. Figure 15a shows a radiograph of a static projectile. This figure shows the projectile configuration prior to loading it into the

cannon. Figure 15b shows two images of the projectile within 1.0 meter of muzzle exit. The direction of flight is left to right; several observations can be made. First, the penetrator is slightly ahead of the sabot; therefore, traction due to frictional forces was sufficient to accelerate the penetrator along with the sabot. Second, the right image shows more rotation of the sabot sections and that the fracture plane was parallel to the axis of symmetry and that complete mechanical disengagement of the sabot from the penetrator has occurred. This radiograph proves conclusively that the concept and analyses were valid.

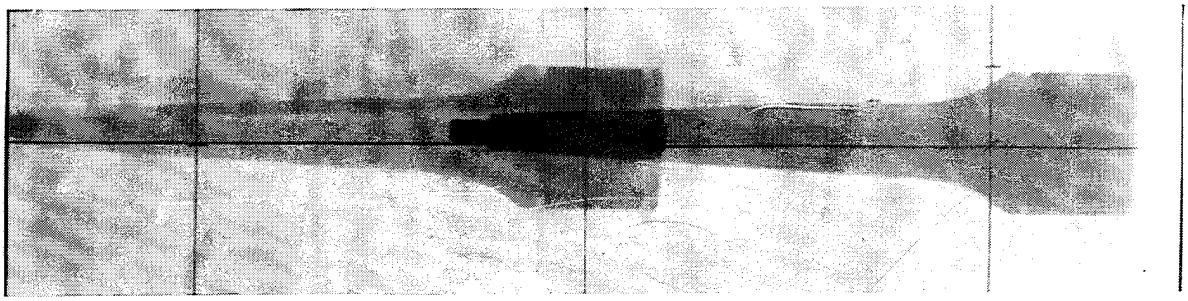

A. Static radiograph of a projectile prior to loading.

B. Radiograph of a projectile at muzzle exit (velocity = 1,650 m/s).

Figure 15. Radiographs of the projectile.

5. CONCLUSIONS

To support the current and future needs of researchers in the area of penetration mechanics, a new concept for the traction launch of subscale KE penetrators has been proposed. By making simplifying assumptions, utilizing free body diagrams and simple physical relationships, a set of governing equations

were developed to specify sabot geometry based on penetrator and cannon geometry. Extensive use of finite element techniques were employed to verify the initial assumptions and concept feasibility.

During the finite element analysis, several different codes were used. In two different analyses, the parametric capabilities of ANSYS were utilized to great advantage in quasi-static solutions. However, ANSYS did not provide adequate means to solve the dynamic solutions. For these problems, NIKE and DYNA were utilized and provided sufficient confidence to continue to the final design. Lastly, comparison of results from quasi-static (ANSYS) to dynamic (DYNA) solutions was exceptional.

Utilization of finite element methods verified the theory presented earlier. However, verification of both the theory and finite element analysis can only be accomplished by actual tests. The outcome of the tests proved that the concept, assumptions, and analysis process were valid.

INTENTIONALLY LEFT BLANK.

6. REFERENCES

DeSalvo, G. J., and R. W. Gorman. "ANSYS Engineering Analysis System User's Manuals." Vol. 1 and 2 (Rev. 4.4a). Swanson Analysis Systems, Inc., Houston, PA.

Drysdale, W. H. "Design of Kinetic Energy Projectiles for Structural Integrity." BRL-TR-02365, U.S. Army Ballistic Research Laboratory, Aberdeen Proving Ground, MD, September 1981.

Hallquist, J. O. "MAZE - An Input Generator for DYNA2D AND NIKE2D." UCID-19029, Lawrence Livermore National Laboratory, Livermore, CA, June 1983.

Hallquist, J. O. "NIKE2D- A Vectorized Implicit, Finite Deformation Finite Element Code for Analyzing the Static and Dynamic Response of 2-D Solids With Interactive Rezoning and Graphics." UCID-19677, Rev.1, Lawrence Livermore National Laboratory, Livermore, CA, December 1986.

Hallquist, J. O. "User's Manual for DYNA2D - An Explicit 2-D Hydrodynamic Finite Element Code with Interactive Rezoning and Graphical Display." UCID-18756, Rev. 3, Lawrence Livermore National Laboratory, Livermore, CA, February 1988.

Oberg, E., F. D. Jones, and H. L. Horton. "Machinery's Handbook, 22nd Edition." New York: Industrial Press Inc., July 1985.

INTENTIONALLY LEFT BLANK.

NO. OF COPIES	ORGANIZATION
2	ADMINISTRATOR ATTN DTIC DDA DEFENSE TECHNICAL INFO CTR CAMERON STATION ALEXANDRIA VA 22304-6145
1	DIRECTOR ATTN AMSRL OP SD TA US ARMY RESEARCH LAB 2800 POWDER MILL RD ADELPHI MD 20783-1145
3	DIRECTOR ATTN AMSRL OP SD TL US ARMY RESEARCH LAB 2800 POWDER MILL RD ADELPHI MD 20783-1145
1	DIRECTOR ATTN AMSRL OP SD TP US ARMY RESEARCH LAB 2800 POWDER MILL RD ADELPHI MD 20783-1145
	ABERDEEN PROVING GROUND
5	DIR USARL ATTN AMSRL OP AP L (305)

NO. OF COPIES	ORGANIZATION
1	HQDA ATTN SARD TT DR F MILTON WASH DC 20310-0103
1	HQDA ATTN SARD TT MR J APPEL WASH DC 20310-0103
1	HQDA ATTN SARD TT MS C NASH WASH DC 20310-0103
1	HQDA ATTN SARD TR DR R CHAIT WASH DC 20310-0103
1	HQDA ATTN SARD TR MS K KOMINOS WASH DC 201310-0103
1	DIRECTOR ATTN AMSRL CP CA D SNIDER USARL 2800 POWDER MILL RD ADELPHI MD 20783
7	DIRECTOR ATTN AMSRL MA P L JOHNSON T CHOU USARL ARSNL ST WATERTOWN MA 02172-0001
4	COMMANDER ATTN SMCAR FSE T GORA E ANDRICOPOULOS B KNUTELSKY A GRAF US ARMY ARDEC PCTNY ARSNL NJ 07806-5000
5	COMMANDER ATTN SMCAR CCH T S MUSALLI P CHRISTIAN K FEHSAL N KRASNOW R CARR US ARMY ARDEC PCTNY ARSNL NJ 07806-5000
1	COMMANDER ATTN SMCAR CCH V E FENNELL US ARMY ARDEC PCTNY ARSNL NJ 07806-5000
1	COMMANDER ATTN SMCAR CCH J DELORENZO US ARMY ARDEC PCTNY ARSNL NJ 07806-5000
2	COMMANDER ATTN SMCAR CC J HEDDERICH COL SINCLAIR US ARMY ARDEC PCTNY ARSNL NJ 07806-5000
11	DIRECTOR ATTN SMCAR CCB C KITCHENS J KEANE T ALLEN J VASILAKIS G FRIAR T SIMKINS V MONTVORI J WRZOCHALSKI G D'ANDREA R HASENBEIN SMCAR CCB R S SOPOK BENET WEAPONS LABS WATERVLIET NY 12189
3	COMMANDER ATTN AMSMI RD W MCCORKLE AMSMI RD ST P DOYLE AMSMI RD ST CN T VANDIVER US ARMY MICOM REDSTONE ARSNL AL 35898
2	US ARMY RESEARCH OFFICE ATTN ANDREW CROWSON J CHANDRA PO BOX 12211 RSRH TRI PK NC 27709-2211
1	US ARMY RESEARCH OFFICE ATTN G ANDERSON PO BOX 12211 RSRH TRI PK NC 27709-2211

NO. OF COPIES	ORGANIZATION
2	PROJECT MANAGER ATTN SFAE AR TMA COL BREGARD C KIMKER TANK MAIN ARMAMENT SYSTEMS PCTNY ARSNL NJ 07806-5000
3	PROJECT MANAGER ATTN SFAE AR TMA MD H YUEN J MCGREEN R KOWALSKI TANK MAIN ARMAMENT SYSTEMS PCTNY ARSNL NJ 07806-5000
2	PROJECT MANAGER ATTN SFAE AR TMA MS R JOINSON D GUZIEWICZ TANK MAIN ARMAMENT SYSTEMS PCTNY ARSNL NJ 07806-5000
1	PROJECT MANAGER ATTN SFAE AR TMA MP W LANG TANK MAIN ARMAMENT SYSTEMS PCTNY ARSNL NJ 07806-5000
2	PROJECT EXECUTIVE OFFICER ATTN SFAE AR PM D ADAMS T MCWILLIAMS ARMAMENTS PCTNY ARSNL NJ 07806-5000
2	COMMANDER ATTN J KELLY B WILCOX ARPA 3701 N FAIRFAX DR ARLINGTON VA 22203-1714
2	COMMANDER ATTN WL FIV A MAYER WRIGHT PATTERSON AFB DAYTON OH 45433
2	DIRECTOR ATTN AMSRL VS W ELBER AMSRL VS S F BARTLETT JR NASA LANGLEY RSRCH CTR MAIL STOP 266 HAMPTON VA 23681-0001

NO. OF COPIES	ORGANIZATION
2	NAVAL SURFACE WARFARE CTR CODE G33 DAHLGREN VA 224488
1	NAVAL RESEARCH LAB ATTN I WOLOCK CODE 6383 WASH DC 20375-5000
1	OFFICE OF NAVAL RSRCH MECH DIV ATTN YAPA RAJAPAKSE CODE 1132SM ARLINGTON VA 22217
1	NAVAL ORDNANCE STATION ATTN D HOLMES CODE 2011 ADVANCED SYSTEMS TECHNOLOGY BR LOUISVILLE KY 40214-5245
1	DIRECTOR ATTN D RABERN MEE 13 MAIL STOP J 576 LANL PO BOX 1633 LOS ALAMOS NM 87545
1	OAK RIDGE NATIONAL LAB ATTN R M DAVIS PO BOX 2008 OAK RIDGE TN 37831-6195
2	BATTELLE PNL ATTN R SHAPEL M SMITH PO BOX 999 RICHLAND WA 99352
6	DIRECTOR ATTN C ROBINSON G BENEDETTI W KAWAHARA K PERANO D DAWSON P NIELAN SNL PO BOX 969 LIVERMORE CA 94550-0096
1	DREXEL UNIVERSITY ATTN ALBERT SD WANG 32ND AND CHESTNUT STS PHILADELPHIA PA 19104

NO. OF COPIES	ORGANIZATION
2	NORTH CAROLINA STATE UNIV ATTN W RASDORF L SPAINHOUR CIVIL ENGR DEPT PO BOX 7908 RALEIGH NC 27696-7908
1	PENNSYLVANIA STATE UNIV ATTN DAVID W JENSEN 223 N HAMMOND UNIVERSITY PARK PA 16802
1	PENNSYLVANIA STATE UNIV ATTN RICHARD MCNITT 227 HAMMOND BLDG UNIVERSITY PARK PA 16802
1	PENNSYLVANIA STATE UNIV ATTN RENATA S ENGEL 245 HAMMOND BUILDING UNIVERSITY PARK PA 16801
1	PURDUE UNIV ATTN CT SUN SCHOOL OF AERO & ASTRO W LAFAYETTE IN 47907-1282
1	STANFORD UNIV ATTN S TSAI DEPT OF AERONAUTICS & AEROBALLISTICS DURANT BLDG STANFORD CA 94305
1	THE UNIV OF TEXAS AT AUSTIN ATTN J PRICE CTR FOR ELECTROMECHANICS 10100 BURNET RD AUSTIN TX 78758-4497
1	ARMTEC DEFENSE PRODUCTS ATTN STEVE DYER 85 901 AVE 53 COACHELLA CA 92236
3	ALLIANT TECHSYSTEMS INC ATTN J BODE C CANDLAND K WARD 5901 LINCOLN DR MINNEAPOLIS MN 55346-1674

NO. OF COPIES	ORGANIZATION
1	CHAMBERLAIN MFG CORP ATTN T LYNCH R&D DIV 550 ESTHER ST WATERLOO IA 50704
1	CHAMBERLAIN MFG CORP ATTN M TOWNSEND R&D DIV 550 ESTHER ST WATERLOO IA 50704
1	CUSTOM ANALYTICAL ENG SYS INC ATTN A ALEXANDER STAR ROUTE BOX 4A FLINTSTONE MD 21530
1	GDLSD ATTN D BARTLE PO BOX 1901 WARREN MI 48090
4	IAT ATTN T KIEHNE S BLESS R SUBRUMANIUM 4030 2 W BRAKER LN AUSTIN TX 78759
1	INTERFEROMETRICS INC ATTN R LARRIVA VP 8150 LEESBURG PIKE VIENNA VA 22100
2	KAMAN SCIENCES CORP ATTN D ELDER T HAYDEN PO BOX 7463 COLORADO SPRINGS CO 80933
3	LORAL VOUGHT SYSTEMS ATTN G JACKSON K COOK L L HADDEN 1701 W MARSHALL DR GRAND PRAIRIE TX 75051
2	MARTIN MARIETTA CORP ATTN P DEWAR L SPONAR 230 EAST GODDARD BLVD KING OF PRUSSIA PA 19406

NO. OF COPIES	ORGANIZATION
1	OLIN CORP ATTN E STEINER PO BOX 127 RED LION PA 17356
1	OLIN CORP ATTN L WHITMORE 10101 9TH ST NORTH ST PETERSBURG FL 33702
2	UNITED DEFENSE LP ATTN P PARA G THOMAS 1107 COLEMAN AVE BOX 367 SAN JOSE CA 95103
	ABERDEEN PROVING GROUND
50	DIRECTOR USARL ATTN AMSRL CI C MERMEGAN 394 AMSRL CI C W STUREK 1121 AMSRL CI CB R KASTE 394 AMSRL CI S A MARK 309 AMSRL SL B P DIETZ 328 AMSRL SL BA J WALBERT 1065 AMSRL SL BL D BELY 328 AMSRL SL I D HASKILL 1065 AMSRL WT P A HORST 390A AMSRL WT PA T MINOR 390 AMSRL WT PB E SCHMIDT 120 P PLOSTINS 120 AMSRL WT PC R FIFER 390A AMSRL WT PD B BURNS 390 W DRYSDALE 390 S WILKERSON 390 R KASTE 390 L BURTON 390 AMSRL WT T W MORRISON 309 AMSRL WT TA W GILLICH 393 W BRUCHEY 393 T HAVEL 393 M KEELE 393

NO. OF COPIES	ORGANIZATION
	AMSRL WT TC R COATES 309 W DE ROSSET 309 R PHILLABAUM 309 T BJERKE 309 L MAGNESS 309 E KENNEDY 309 R MUDD 309 B SORENSEN 309 (10 CPS) AMSRL WT W C MURPHY 120 AMSRL WT WA B MOORE 394 A BARAN 394 AMSRL WT TD T FARRAND 309 K FRANK 309 G RANDERS-PEHRSON 309 AMSRL WT WB F BRANDON 120 W D'AMICO 120 AMSRL WT WC J ROCCHIO 120 AMSRL WT WE J TEMPERLEY 120

INTENTIONALLY LEFT BLANK.

USER EVALUATION SHEET/CHANGE OF ADDRESS

This Laboratory undertakes a continuing effort to improve the quality of the reports it publishes. Your comments/answers to the items/questions below will aid us in our efforts.

1. ARL Report Number ARL-TR-798 Date of Report July 1995

2. Date Report Received _____

3. Does this report satisfy a need? (Comment on purpose, related project, or other area of interest for which the report will be used.) _____

4. Specifically, how is the report being used? (Information source, design data, procedure, source of ideas, etc.) _____

5. Has the information in this report led to any quantitative savings as far as man-hours or dollars saved, operating costs avoided, or efficiencies achieved, etc? If so, please elaborate. _____

6. General Comments. What do you think should be changed to improve future reports? (Indicate changes to organization, technical content, format, etc.) _____

CURRENT ADDRESS

_____
Organization

_____
Name

_____
Street or P.O. Box No.

_____
City, State, Zip Code

7. If indicating a Change of Address or Address Correction, please provide the Current or Correct address above and the Old or Incorrect address below.

OLD ADDRESS

_____
Organization

_____
Name

_____
Street or P.O. Box No.

_____
City, State, Zip Code

(Remove this sheet, fold as indicated, tape closed, and mail.)
(DO NOT STAPLE)

DEPARTMENT OF THE ARMY

OFFICIAL BUSINESS

NO POSTAGE
NECESSARY
IF MAILED
IN THE
UNITED STATES

BUSINESS REPLY MAIL
FIRST CLASS PERMIT NO 0001,APG,MD

POSTAGE WILL BE PAID BY ADDRESSEE

DIRECTOR
U.S. ARMY RESEARCH LABORATORY
ATTN: AMSRL-WT-TC
ABERDEEN PROVING GROUND, MD 21005-5066